

RESEARCH ARTICLE

10.1002/2015JD023072

Key Points:

- Snowfall amounts at Summit are a factor of 3 larger in summer relative to winter
- Precipitation is dominated by conditions with moist, southerly winds
- Ice-phase precipitation processes are quite important at Summit

Correspondence to:

M. D. Shupe,
Matthew.Shupe@noaa.gov

Citation:

Castellani, B. B., M. D. Shupe, D. R. Hudak, and B. E. Sheppard (2015), The annual cycle of snowfall at Summit, Greenland, *J. Geophys. Res. Atmos.*, 120, 6654–6668, doi:10.1002/2015JD023072.

Received 5 JAN 2015

Accepted 17 JUN 2015

Accepted article online 21 JUN 2015

Published online 14 JUL 2015

The annual cycle of snowfall at Summit, Greenland

Benjamin B. Castellani¹, Matthew D. Shupe¹, David R. Hudak², and Brian E. Sheppard²

¹Physical Sciences Division, Cooperative Institute for Research in Environmental Science and NOAA Earth System Research Laboratory, Boulder, Colorado, USA, ²Environment Canada, King City, Ontario, Canada

Abstract While snow accumulation over central Greenland has been extensively studied, interannual variability of snowfall in the region is not well understood due to a dearth of observations. The Integrated Characterization of Energy, Clouds, Atmospheric state and Precipitation at Summit (ICECAPS) project at Summit, Greenland, offers a unique, ground-based opportunity to study precipitation in central Greenland where the surface mass balance is positive. Combining data from a Precipitation Occurrence Sensor System (POSS), Millimeter-wavelength Cloud Radar (MMCR), and snow stake field, the annual cycle of precipitation at Summit is examined. Average daily snowfall is higher by a factor of 3 from June to October compared to November to May, while surface height change is only higher by 15% during the same timeframes. This reduced variability in surface height is explained by the seasonally varying nature of latent heat flux, compaction, and wind contributions. The ICECAPS remote sensors and stake field measurements do not agree as far as total annual water equivalent. This discrepancy is likely due to a low bias in the POSS and MMCR snowfall retrievals for Summit. To further examine the seasonal cycle, snowfall measurements by the POSS were linked to local meteorological parameters, including wind direction, liquid water path (LWP), 2 m temperature, and precipitable water vapor. An observed wind direction and moisture dependence are consistent with snowfall being linked to pulses of moist air that originate over nearby, ice-free ocean, a resource that becomes more readily available in summertime as the winter sea ice retreats. LWP is shown to have little relationship to snowfall, indicating that ice-phase precipitation processes are quite important for snowfall at Summit.

1. Introduction

The Greenland Ice Sheet (GIS) is made up of nearly $3 \times 10^6 \text{ km}^3$ of ice, which if melted would raise the global mean sea level 6–8 m [Ohmura and Reeh, 1991; Alley et al., 2005; Gregory and Huybrechts, 2006] and would inject substantial fresh meltwater into the North Atlantic Ocean, impacting the global thermohaline circulation [Rahmstorf, 1995, 2000; Fichefet et al., 2003; Stouffer et al., 2006]. In general, over the year, net melting is seen on the edges of the GIS, while slight net accumulation occurs in the interior [Krabill et al., 2000]. The latest estimates indicate the overall negative mass balance of the GIS has contributed around 8 mm to sea level rise for the period 1992–2011 and the rate is increasing [van den Broeke et al., 2009; Shepherd et al., 2012]. While much of the current research is focused on the melting coastal areas, a more complete understanding of the positive mass balance in the interior regions of the GIS, especially the seasonal and inter-annual variability, is essential for diagnosing Greenland's net contribution to sea level rise.

New measurements can help fill some important knowledge gaps regarding the central GIS mass balance. Recently the Integrated Characterization of Energy, Clouds, Atmospheric state and Precipitation at Summit (ICECAPS) project launched at Summit, Greenland (72.6°N, 38.5°W; 3260 m above sea level), a research site located near the apex of the GIS in a region where the mass balance is thought to be near equilibrium or slightly positive [Thomas et al., 2000]. The overarching goal of the project is to examine how clouds and atmospheric state impact the mass and energy balances of the GIS through the use of ground-based remote sensing instruments [Shupe et al., 2013]. This project commenced in the summer of 2010 and is a collaborative effort between several universities and agencies. Included in the instrumentation are two depolarization lidars, a ceilometer, a millimeter-wave cloud radar, a precipitation occurrence sensor system, two microwave radiometers, a spectral infrared interferometer, a sodar, a sky imager, radiosondes, and periodic ice crystal imaging. ICECAPS offers an unrivaled opportunity to study snowfall in the center of the GIS because of the vast array of complementary, co-located, ground-based remote-sensing instruments and the project's prolonged measurement period for understanding the interactions among clouds, atmospheric state, and precipitation.

This paper focuses on ICECAPS measurements that are useful for characterizing precipitation. The first objective is to evaluate the ICECAPS snowfall measurements against each other to gauge the uncertainty associated with the measurements and retrievals. Then, using these measurements, the annual cycle of precipitation at Summit is presented and compared to independent measurements from a snow stake field. Finally, snowfall is examined in the context of local meteorological conditions to better understand the sources of precipitation.

2. Instrumentation

Numerous data sets from several instruments are utilized to understand the precipitation at Summit. A brief description of these particular instruments follows.

2.1. Precipitation Occurrence Sensor System

The Precipitation Occurrence Sensor System (POSS) [Sheppard and Joe, 2008] is a bistatic, continuous-wave, X-band (wavelength of 2.85 cm) Doppler radar that was originally developed by the Meteorological Service of Canada for the observation of precipitation occurrence, rate, and type. The transmitter and receiver are separated by 45 cm and are both pointed upward, angled 20° from vertical, with an approximate sampling volume of one cubic meter located around their intersecting sight lines. The POSS measures the Doppler velocity spectrum of any hydrometeors in its sampling volume. The POSS has mainly been used since the early 1990s for liquid precipitation applications [Sheppard, 1990; Sheppard and Joe, 1994, 2008; Campos and Zawadzki, 2000] but, to a lesser extent, has been used for solid precipitation as well [Sheppard and Joe, 2000, 2008; Shiina et al., 2010].

2.2. Millimeter-Wave Cloud Radar

The Millimeter-wave Cloud Radar (MMCR) [Moran et al., 1998], which operates at 35 GHz and has Doppler capability, measures the backscattered power and Doppler spectrum of scatterers for a profile of range gates in the vertical and is used to detect cloud presence, boundaries, and phase [Shupe, 2007]. Radar reflectivity can be derived from the backscattered power and is roughly proportional to the water equivalent diameter to the sixth power, summed over the size distribution, assuming the scatterers meet the Rayleigh criteria. The MMCR self-calibrates the entire system, except the antenna, on a monthly basis and has a nominal uncertainty in reflectivity of 1 dB (K. Moran, personal communication, 2014). Reflectivity and snowfall measurements from the MMCR will be compared to those from the POSS.

2.3. Snow Stake Field

To provide an additional perspective on the mass balance at Summit, the data from a nearby snow stake field are incorporated into this analysis. The stake field is a 10 × 10 grid of bamboo stakes with 8 m spacing outfitted with measurement markings. The field is located in a remote, undisturbed location within 1 km of the ICECAPS measurements and is used to measure changes in the height of the snow surface (hereafter referred to as surface height change [Dibb and Fahnestock, 2004]). Roughly once per week, a measurement is taken by an observer at each stake in the field to a precision of 0.1 cm (lower precision for the earlier part of the data set). The field provides the longest standing semi-real-time surface height change record at Summit stretching back 10 years to 2003. Excluding human subjectivity or error, most variability in this data set comes from drifting and blowing snow. Often many of the stakes will see opposing height changes during the same week. To reduce this error, all 100 stakes are averaged to give a single value for each measurement period. These data are not directly associated with the ICECAPS project and are used to provide an additional perspective in section 5.1.

2.4. Microwave Radiometers

Two microwave radiometers are present at Summit that passively measure downwelling atmospheric microwave radiation. The Humidity and Temperature Profiler microwave radiometer [Rose et al., 2005] operates at numerous channels ranging from 22 to 58 GHz, while the High-Frequency Microwave Radiometer operates at 90 and 150 GHz. Measurements from 20 to 31 GHz are used to derive the column-integrated precipitable water vapor (PWV) [Turner et al., 2007], while measurements from 23, 31, 90, and 150 GHz are used to derive the column-integrated liquid water path (LWP) [Liljegren, 1999; Turner et al., 2007]. These

parameters play an important role in relating the snowfall measurements by active sensors to the local atmospheric state.

2.5. Temporary Atmospheric Watch Observatory

The NOAA Earth System Research Laboratory Global Monitoring Division has had a presence at Summit since the mid-1990s. Currently their Temporary Atmospheric Watch Observatory (TAWO) includes measurements of 2 m temperature and relative humidity, 10 m wind speed and direction, and 10 m temperature and station pressure. Several of these measurements will be used in the analysis contained in section 5.2. TAWO is not directly associated with the ICECAPS project.

3. Radars and Snowfall

3.1. Data

Radars have been used to examine precipitation processes for many years. Using radar for solid precipitation is more challenging because snowflakes come in many forms, with widely varying sizes and habits (geometric shapes), which all have unique and complex scattering properties [Fujiyoshi *et al.*, 1990; Matrosov, 1992; Macke *et al.*, 1996; Liu, 2008]. This variation serves as a major source of uncertainty for snowfall retrievals from radar measurements and has been a topic of research by radar meteorologists for decades in both identifying which habits are occurring and the associated scattering properties. Fortunately, improvements in computational power have allowed scattering codes, such as the T-matrix method [Mischenko, 2000] and the discrete dipole approximation [Purcell and Pennypacker, 1973], to model the backscatter properties of intricate nonspherical particles. However, a remaining challenge is to identify the appropriate crystal types in order to apply the appropriate scattering approximations when conducting snowfall retrievals. Crystal type can vary significantly from location-to-location, storm-to-storm, or even hour-to-hour at a single location.

The POSS is a vital component to understanding the snowfall at Summit. One important data set used from this instrument is the equivalent reflectivity factor, Z_e (hereafter, reflectivity). Due to several factors specific to the POSS, it does not directly measure Z_e . However, using the T-matrix approach, Z_e can be estimated from the POSS spectral zeroth moment [Sheppard and Joe, 2008].

While the POSS samples about 1 m^3 of atmosphere located a few meters above ground level (agl), the MMCR is a pulsed radar system that measures a vertical profile of true reflectivity. Sample volumes are on the order of hundreds of cubic meters, with the lowest reliable range gate located near 200 m agl. In order to choose the measurements that best represent precipitation at the surface, the reflectivity values in the lowest reliable MMCR range gate are used. This provides the best guess as to what is actually reaching the ground, under the assumption that the reflectivity will be relatively constant down to the surface on average [Matrosov *et al.*, 2008].

During a portion of the measurement period, a saturation issue impacted the data in the lowest MMCR range gates, wherein the input signal was too strong for the detector. This occurred as the result of a component failure that shifted the dynamic range of the detector toward lower powers. This issue affected the lowest several range gates and caused the MMCR to underestimate the reflectivity in these lower gates during events of moderate to heavy snowfall. A correction was applied to data where saturation was deemed to be occurring, wherein the height selected to best represent the surface precipitation was above the gates impacted by saturation, and could be as high as 700 m agl, instead of the usual 200 m agl.

3.2. Snowfall Retrievals

Radar reflectivity is often related to water equivalent (w.e.) snowfall rate, S , through equations known as Z_e - S relationships, which have the general power law form, $Z_e = B S^\beta$, where B and β are coefficients and S has units of mm w.e. h^{-1} . These coefficients are not fixed and can vary significantly based on crystal habits and the snow size distribution. Thus, no one set of coefficients is generally applicable. Z_e - S relationships are more complicated for snow than for rain due to uncertainties in crystal habit, orientation, fall velocity, density, degree of riming, size, and the impacts all of these have on the scattering properties.

For this analysis, the Z_e - S relationships used with MMCR and POSS measurements were developed using the T-matrix scattering model [Mischenko, 2000] to approximate the backscattering properties of the snowflakes

[Matrosov, 2007; Matrosov et al., 2009]. By making assumptions about the characteristics of the snowflake size distribution, both a theoretical reflectivity and snowfall rate can be determined, as well as their power law relationship to one another. The resulting relationships will vary based on the assumptions.

Due to the hydrometeor size dependence of the POSS's sampling volume, the 0th moment (P_0) of the measured Doppler spectrum is not linearly related to Z_e . This makes determining S more of a challenge than for a pulsed radar system like the MMCR. A second-order regression of $\log(S)$ on $\log(P_0)$ is used to find S [Sheppard and Joe, 2008]. This method is unique to the POSS but is equivalent to Z_e - S methods for other radars such as the MMCR. More details on this POSS retrieval are given in Sheppard and Joe [2008]. Due to several effects, including the influence of wind and radome wetting, the POSS has been shown to have an "undercatch" for solid precipitation with median catch ratio of 0.90 and an interquartile range of -0.17 to $+0.24$ around the median when compared to Double Fenced Intercomparison Reference snow gauges [Sheppard and Joe, 2008; Wong, 2012]. To adjust for this median undercatch, the standard POSS snowfall retrieval is adjusted by a factor of 1.11. MMCR-based snowfall retrievals follow many of the same principles; however, since the MMCR is a pulsed system, a Z_e - S relationship for dry snow described and developed by Matrosov [2007] under a basic set of assumptions for millimeter wavelengths is used to derive snowfall rate according to $Z_e = 56 S^{1.20}$.

The MMCR's operation during the measurement period was intermittent at times. For this reason, the POSS is the primary instrument considered here, but it will be compared to, and supplemented by, measurements from the MMCR.

4. Evaluation of Methods

The objective here is to evaluate and compare the POSS and MMCR measurements and retrievals for consistency with regard to reflectivity and snowfall. The POSS has been collecting data at Summit since September of 2010 with $>99\%$ uptime. Unfortunately, no independent precipitation gauges exist at Summit to directly evaluate the POSS snowfall retrievals at the surface. However, the MMCR, which was operational periodically through the time period, can be used as an independent evaluation of POSS reflectivities. The equivalent reflectivity derived from the POSS (Z_{EP}) is compared to the equivalent reflectivity measured by the MMCR (Z_{EM}), an instrument with a relatively well-tracked and characterized calibration when it is operating properly. This intercomparison provides some baseline evaluation of the POSS calibration, as well as the assumptions that go into the scattering code used to develop the retrievals for both instruments.

The POSS and MMCR operate in different radar bands, with wavelengths of 2.85 cm and 8.5 mm, respectively. This difference causes dissimilarities in the way the radar beams interact with larger snowflakes. For centimeter wavelengths, the Rayleigh approximation holds well for particle sizes of up to 4 or 5 mm [Matrosov et al., 2009]. However, for the millimeter-scale wavelength of the MMCR, scattering from particles of this size can deviate significantly from Rayleigh theory. The derivation of Z_e for the POSS is calculated from Mie theory and makes no assumptions about particle size. For particles smaller than a couple of millimeters, the Ka-band reflectivities will be smaller by a few decibel or less [Matrosov, 1998] and even less for the dry snowflakes at Summit [Matrosov, 2007]. Based on qualitative on-site ice crystal images, most snowflakes at Summit are relatively small and fall below these thresholds. However, the potential contributions of non-Rayleigh effects to differences in reflectivity between these instruments get larger for increasing particle sizes (and higher Z_e).

Due to the measurement height difference between the POSS and MMCR, which may range from 200 to 700 m, a time lag of 10 min is introduced for comparing the two instruments to account for the time it takes ice crystals to fall from those heights to the surface. To further reduce the uncertainty in time and space, the data for both instruments were averaged temporally. Averaging windows ranging from 1 min up to 1 h were evaluated, and 10 min was chosen as the best compromise between statistical representation and temporal resolution.

The POSS and MMCR reflectivities are compared by considering the instantaneous difference, ΔZ (Figure 1a). This comparison is useful for evaluating the model-derived regressions used for calculating the POSS reflectivity. Consequently, since the same formalism and assumptions are used to derive snowfall rate from the POSS, the evaluation may also inform some of the uncertainties in that retrieval. The bolded black

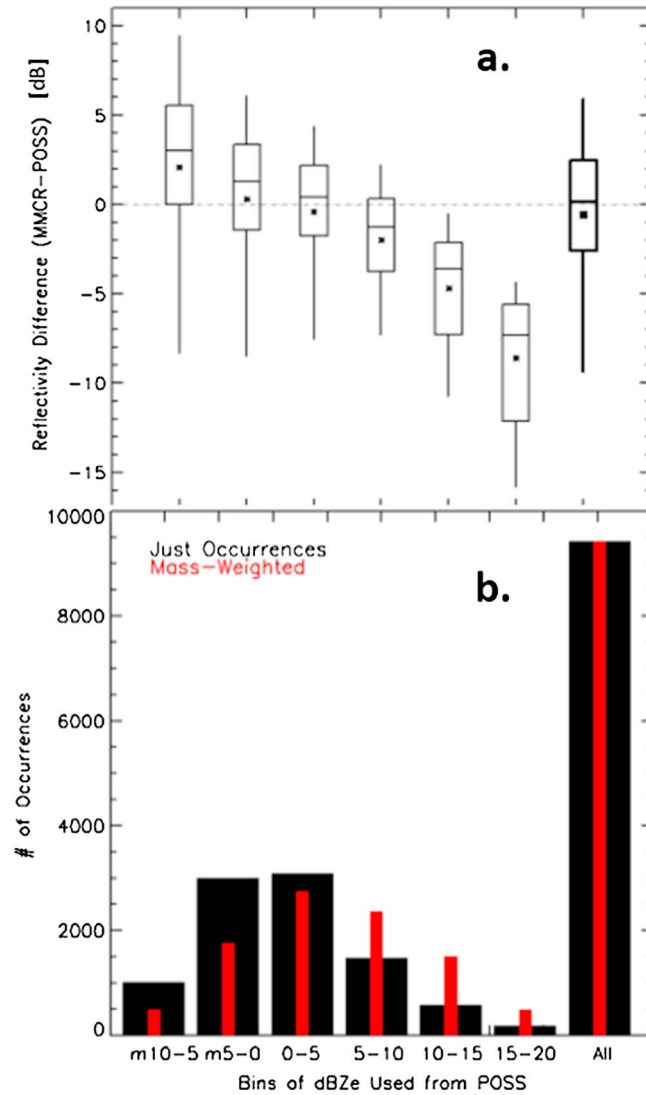


Figure 1. (a) Box-and-whisker plots of the reflectivity difference between MMCR and POSS, ΔZ , for all data (bolded plot on the right) and for various Z_{EP} bin subsets (six plots on the left). (b) Bar graph showing the number of occurrences that fall into each Z_{EP} bin (black) and the relative mass-weight occurrence in each bin (red).

box-and-whisker plot on the far right of Figure 1a contains all of the data. The POSS-derived reflectivity compares adequately with the MMCR, showing approximately no median bias and a mean bias of -0.6 dB (POSS lower than MMCR). Here we evaluate the distribution of differences between POSS and MMCR, σ_{TOT} , expressed as a standard deviation, by considering the individual components that might contribute to the differences, using

$$\sigma_{TOT} = \sqrt{(\sigma_{MMCR}^2 + \sigma_{POSS}^2 + \sigma_{COMP}^2)}, \quad (1)$$

where σ_{MMCR} is the uncertainty associated with the MMCR reflectivity and has a known nominal value of 1 dB, σ_{POSS} is the effective uncertainty of POSS reflectivity that includes both the POSS calibration uncertainty and the uncertainty contributed by the regressions for determining the true POSS reflectivity, and σ_{COMP} is the contribution introduced from differences in sampling volumes and time. Rearranging equation (1) and solving for σ_{POSS} gives an estimate of POSS uncertainties:

$$\sigma_{POSS} = \sqrt{(\sigma_{TOT}^2 - \sigma_{COMP}^2 - \sigma_{MMCR}^2)}. \quad (2)$$

Based on all 3 years of data (the bolded box and whisker plot in Figure 1a), σ_{TOT} is equal to 5.3 dB. Thus, the maximum possible uncertainty of the POSS (i.e., assuming no differences due to sample volume and $\sigma_{COMP} = 0$) is 5.2 dB. However, we have summarized several notable complications with the comparison. One of the most influential is likely the difference between the two

sampling volumes. The MMCR measures a comparatively large volume a few hundred meters off the ground, while the POSS is just a few meters above the surface measuring a small volume about 1 m^3 in size. The degree to which the POSS and MMCR measure the same general aspects of the snowfall depends on the horizontal wind speed, the homogeneity of the distribution of snow on the local scale, and even the properties of the snowflakes themselves that impact their fall speed, which determines the time lag before the snow at the height of the MMCR observations makes it to the height of the POSS observations. These differences due to sampling volume likely contribute significantly to the overall variability in observed differences in reflectivity.

While these conditions cannot be fully characterized, Figure 2 gives insight into potential contributions to observed differences by characterizing temporal differences between 10 min averaged bins of POSS and MMCR data and 10 min averaged bins of the same data that were offset by 1, 3, 5, and 10 min. Essentially, this is a proxy for how much reflectivity changes in time and can shed light on the variability of data expected by potential temporal offsets between POSS and MMCR sample volumes. At the top of each box-and-whisker in the figure, the standard deviation is shown. With a 3 or 5 min offset, the standard deviation is already near

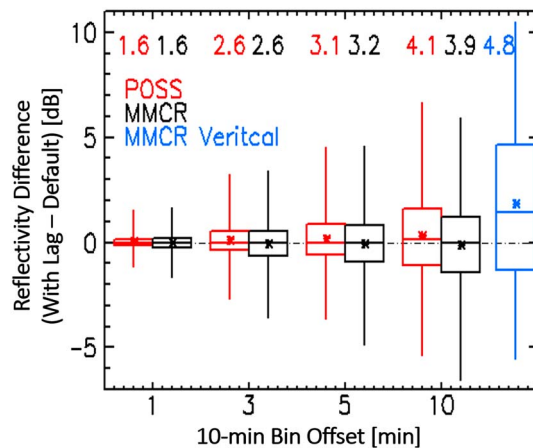


Figure 2. Box-and-whisker plots showing difference statistics of 10 min averaged reflectivities relative to 10 min averaged reflectivities from the same data set that are simply offset by 1, 3, 5, and 10 min for the POSS (red) and MMCR (black). These results illustrate the potential variability associated with choosing slightly different time windows for comparing the POSS and MMCR reflectivities. The blue box-and-whisker plot on the right has no bin offset and simply represents the difference between the MMCR reflectivities at 200 m and 700 m agl. The values near the top of the figure show the standard deviation of data in each column.

3 dB. It is important to note that both instruments show basically the same temporal self-variance statistics, suggesting that this variability is likely related to how snowfall varies and is independent of the instruments. The blue box-and-whisker represents the difference between reflectivity measured by the MMCR at 200 m and 700 m during times when snowfall was occurring and serves as a proxy for the potential vertical variation in reflectivity that could impact the comparison. The positive bias (i.e., reflectivity at 200 m being larger) suggests, on average, a net growth of snowflakes as they fall toward the surface. The standard deviation representing vertical variability across this 500 m was found to be 4.8 dB.

Even though the overall uncertainty of the POSS reflectivity was found to have an upper limit of 5.2 dB, the uncertainty

associated with the time-space comparison alone can easily range between 3 and 5 dB. This gives more confidence to the POSS's calibration and regressions. As a result of this information, the POSS is likely to be accurate to within 3 dB (i.e., a factor 2), if not better. This estimate is close to the 2.9 dB standard deviation found by Huang *et al.* [2015], who analyzed Z_e differences between the POSS and a 2-D video disdrometer for snowfall.

Returning to Figure 1a, the six leftmost black box-and-whisker plots show reflectivity differences as a function of reflectivity (subset by ranges of Z_{EP}). At lower reflectivities, the POSS tends to measure lower reflectivities than the MMCR. Moving toward higher reflectivities, the MMCR begins to measure increasingly lower reflectivities than the POSS. This trend has a few potential explanations. The likely culprit is the introduction of non-Rayleigh effects to the shorter-wavelength MMCR at higher reflectivities due to the larger particle sizes. Also, the MMCR saturation issue may not be fully accounted for in all situations. As mentioned, saturation only affects the MMCR at times of higher reflectivity, and it does so by lowering the measured MMCR reflectivity. Both of these effects would contribute in the manner observed in Figure 1a. The apparent negative POSS bias at low Z_{EP} is likely related to the small sampling volume and minimum detectable signal of the POSS. Most of the data fall within Z_{EP} bins that have mean and median differences less than 3 dB. In total, 93% of the snowfall events and 78% of snowfall mass are within these bins (Figure 1b). Overall, the POSS measurements compare adequately with the MMCR for their overlapping measurement periods, giving confidence in the measurement quality of both instruments.

A point-to-point comparison of instantaneous snowfall rates derived from the respective reflectivities shows that a large portion of the data follows the one-to-one line (Figure 3) with a correlation of 0.75 and a modest root mean squared error of 0.08 mm/h. Despite the POSS appearing to have lower measurements of reflectivity than the MMCR at the smallest reflectivities, the opposite is true for snowfall rate (i.e., at the smallest snowfall rates, the POSS rates are higher). This is due to differences in the way the Z_e -S relationships are developed for these two radar systems.

5. Results and Discussion

5.1. Annual Cycle of Snowfall

One basic, but extremely valuable piece of information is the annual cycle of snowfall in the central GIS. Figure 4a shows this annual cycle through monthly means for the POSS (September 2010 to October 2013) and MMCR (intermittent for September 2010 to October 2013) along with surface height changes from the stake field.

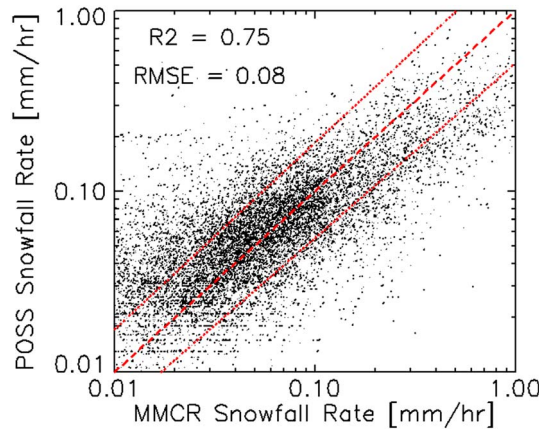


Figure 3. Scatterplot of POSS and MMCR snowfall rates for all times that both instruments were actively measuring snowfall. The dashed red line is the one-to-one line, and the dotted red lines show a factor of 2 difference.

Unlike the instantaneous measurements taken by the POSS and MMCR, the stake field only provides three to five measurements per month.

The annual snowfall cycle indicated by the POSS and MMCR is defined by a large summertime peak in June–September, with lesser snowfall throughout the rest of the year. The annual minimum occurs in springtime. July sees the most snowfall, averaging 18.9 mm w.e. from the POSS. March–May receives the lowest amount relative to the rest of the year, only averaging 3.3 mm/month. The mean annual snowfall over the time period from the POSS (MMCR; differing time period) is 92.5 (88.8) mm w.e., with 61% (49%) occurring in June–September. The

annual value of 92.5 mm w.e. for the POSS has a potential spread due to uncertainty in the undercatch ratio of 81.1 to 126.7 mm w.e. The largest monthly variability occurs in May, June, and September, where the difference between the maximum and minimum monthly snowfall totals is more than 8 mm w.e., while the rest of the months see a range of variability between 3 and 7 mm w.e. There are monthly differences, generally less than 30% between most monthly means, with MMCR larger during lower snowfall months and POSS larger during

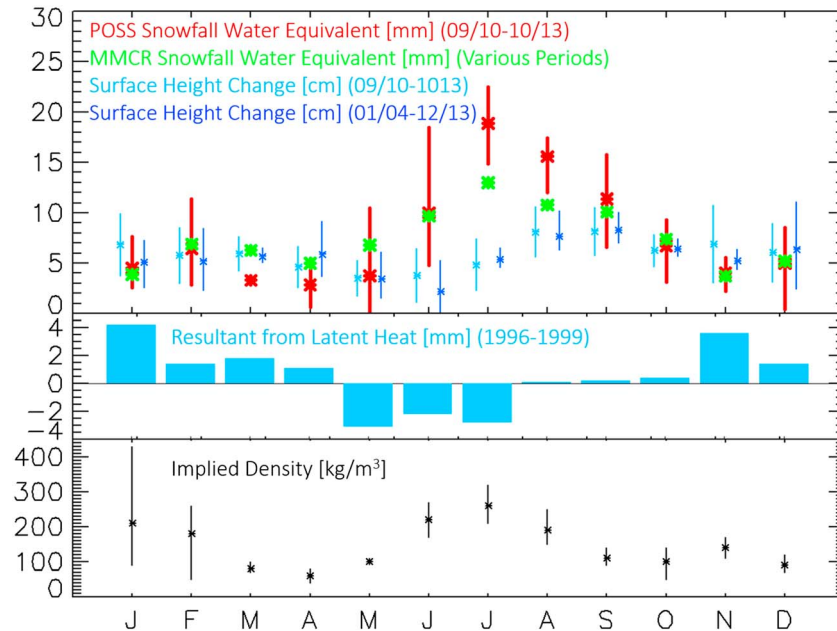


Figure 4. (a) The annual cycle of monthly snowfall at Summit measured by the POSS for September 2010 to October 2013 (red) and the MMCR for a subset of the period (green). The annual cycle of surface height change is given for the same period as the POSS (dark blue) and for January 2004 to December 2013 (light blue). The asterisks indicate the monthly mean values for all data sets. For the short-term data, the extent of the vertical lines indicates the maximum and minimum monthly values during the period. For the 10 year surface height change data set, the extent of the vertical lines indicates ± 1 standard deviation from the monthly mean. (b) The annual cycle of deposition due to latent heat flux for Summit from April 1996 to August 1999, constructed from Table 5 of Box and Steffen [2001]. (c) The monthly density of the solid accumulation implied by surface height change, POSS snowfall, and latent heat contribution measurements, assuming no other contributing factors. The asterisks indicate monthly mean values, while the extent of the vertical lines indicates maximum and minimum monthly values during the three-year period.

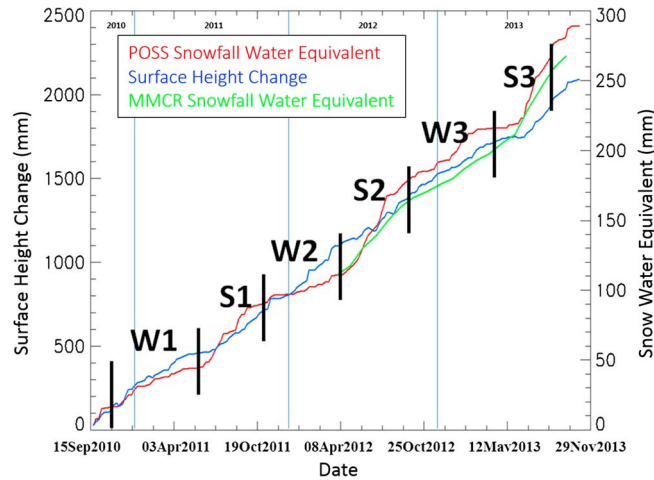


Figure 5. Cumulative comparison between POSS snowfall (red), MMCR snowfall (green), and surface height change (blue) for the overlapping measurement period from September 2010 to October 2013 represented in terms of total snowfall or height change since 15 September 2010. The vertical blue lines designate 1 Jan of the calendar year shown. The vertical black lines and alphanumeric headings define the time periods that are referred to in Table 1. Note the separate axes for (left) surface height change and (right) snowfall.

higher snowfall months, likely related to the differences discussed in section 4 and Figure 1. Despite the varying temporal coverage and differing snowfall retrievals, the POSS and MMCR snowfall annual cycles compare well overall.

The measured monthly surface height change over the same time period also shows seasonal variability, although the maxima and minima are not in sync and the amplitude is smaller. Surface height change peaks in August and September, measuring 7.7 cm and 8.3 cm, respectively. A spring minimum is observed, with the lowest monthly mean height change occurring in June (2.2 cm). Each monthly mean of surface height change over the measurement period falls within one standard deviation of the 10 year monthly mean height change, suggesting that the 3 year data set is approximately representative of

the height change over the last decade. Over the entire 10 year period, the mean annual height change was 71 ± 11 cm. This value compares well with *Bales et al.* [2001] who found an average annual solid accumulation of 69 cm for the period of 1904 to 1974 and *Dibb and Fahnestock* [2004] who measured an annual mean solid accumulation of 65 cm for the periods of August 2000 to August 2002 and 1991 to 1995 based on accumulation field data.

To further understand the relationship between snowfall and surface height change, cumulative series of both data are plotted in Figure 5. Note the differing axes for height change and snowfall. Snowfall and height change qualitatively track each other quite well throughout the time period with small seasonal differences in slope related to modest seasonal differences in compaction and snow density [e.g., *Dibb and Fahnestock*, 2004]. The rate of surface height change throughout the measurement period is relatively constant, which agrees with the findings of *Steffen and Box* [2001] and *Dibb and Fahnestock* [2004] for Summit. The snowfall rate, on the other hand, appears more akin to a step function, with minimal snowfall for a little more than half the year in the winter months (Periods W1, W2, and W3) and increased snowfall in the summer periods (Periods S1, S2, and S3). For consistency purposes, the MMCR cumulative snowfall is shown in Figure 5 for the time period when the data were reliable and continuous. Over that year and a half, the MMCR measured about 20 mm w.e. less snowfall than the POSS.

Mean annual statistics are useful to quantify the major difference in amplitude between snowfall and surface height change (Table 1). In general, the months of June through October can be defined as the summer snowy season. The snowfall rate in the snowy season is $0.40 \text{ mm w.e. d}^{-1}$, three times larger than the rest of the year. The surface height change rate during the snowy season is 2.0 mm d^{-1} , only about 15% larger than during the rest of the year.

To examine these seasonal differences in snowfall and surface height change, we first qualitatively define surface height change, ΔH , as the measured change in the height of the snow surface in cm, according to

$$\Delta H = P + L - C + W, \tag{3}$$

where P is snowfall, L is the net contribution from latent heat flux (can be positive (deposition) or negative (sublimation)), C is compaction, and W is the influence of snow redistribution by the wind and can be positive or negative. Despite the fact that snowfall generally dominates the surface mass balance in central Greenland [*Fettweis*, 2007; *Etema et al.*, 2009], the overall correlation between POSS snowfall and ΔH from Figure 5 is 0.39. This relatively low correlation with snowfall suggests that other factors in equation (3) may

Table 1. Snowfall and Surface Height Change Data for Summer and Winter Periods During the Record of POSS Measurements

| Time Period ^a | Period Label | Total Days | Total Snow (mm w.e.) | | Snow Rate (mm w.e. d ⁻¹) | | Total Surface Height Change (mm) | Rate of Surface Height Change (mm d ⁻¹) |
|---------------------------|--------------|------------|----------------------|------|--------------------------------------|------|----------------------------------|---|
| | | | POSS | MMCR | POSS | MMCR | | |
| 1 Nov 2010 to 31 May 2011 | W1 | 212 | 27.8 | - | 0.13 | - | 349 | 1.6 |
| 1 Jun 2011 to 31 Oct 2011 | S1 | 153 | 45.6 | - | 0.30 | - | 257 | 1.7 |
| 1 Nov 2011 to 31 May 2012 | W2 | 212 | 30.2 | - | 0.14 | - | 407 | 1.9 |
| 1 Jun 2012 to 31 Oct 2012 | S2 | 153 | 65.0 | 49.5 | 0.42 | 0.32 | 331 | 2.1 |
| 1 Nov 2012 to 31 May 2013 | W3 | 212 | 31.0 | 38.6 | 0.15 | 0.18 | 333 | 1.6 |
| 1 Jun 2013 to 31 Oct 2013 | S3 | 153 | 71.8 | 62.1 | 0.47 | 0.41 | 321 | 2.1 |
| Mean (winter) | W | 212 | 29.7 | 38.6 | 0.14 | 0.18 | 363 | 1.7 |
| Mean (summer) | S | 153 | 60.8 | 55.8 | 0.40 | 0.36 | 303 | 2.0 |

^aThe beginning and end of each period were subjectively chosen based on distinct regimes of snowfall rate visible in Figure 5. The mean values for the summer (S) and winter (W) periods are also shown.

be important at short time scales. The latent heat flux contribution, wind redistribution, compaction, or a combination thereof play an influential role that varies seasonally.

In the summer months, when snowfall is at its peak, the net latent heat flux at Summit is negative or very small (i.e., net sublimation to the atmosphere, see Figure 4b [Box and Steffen, 2001]). Compaction, including the influences from destructive snow metamorphism and firn deflation, increases with increasing surface temperature [Spencer et al., 2001; Steffen and Box, 2001; Arthern et al., 2010]. Both of these factors would counteract the summertime snowfall maximum to lessen its impact on ΔH [Dibb and Fahnestock, 2004]. Another result of these counteracting factors is that the annual peak in ΔH is notably delayed by two months, into September, relative to the snowfall peak which occurs in July. In June and July, when snowfall starts to increase, latent heat flux is negative and significant compaction of the wintertime accumulation occurs due to the warming temperatures. By the end of summer, in August and September, snowfall is still large. However, latent heat flux is no longer negative and the initial large rate of compaction has diminished. This allows for ΔH to increase and peak, even though snowfall is already trending downward. In the winter (October through April), the net latent heat flux is often positive (i.e., net deposition onto the surface [Box and Steffen, 2001]) and compaction is reduced as a result of the lower temperatures. Both of these would explain ΔH being large relative to snowfall in winter, as seen in Figure 4a.

Figure 4c shows the monthly mean implied snowpack density, ρ_i , derived by combining the snowfall and ΔH measurements with the estimates of latent heat flux. The ρ_i is generally less than 300 kg m^{-3} , except in January, which has seen widely varying ρ_i up to 430 kg m^{-3} . The annual average implied density is 145 kg m^{-3} , which is far too low considering the density profile at Summit in the upper meter of snow typically ranges from 300 to 450 kg m^{-3} [Albert and Shultz, 2002; Jacobi et al., 2004; Dibb and Fahnestock, 2004]. Stated in other terms, the mean snowfall of 92.5 mm w.e. observed by the POSS, which is consistent with MMCR-based estimates, is significantly smaller than the mean accumulation of 210 mm w.e. that would result from a modestly low assumed density of 300 kg m^{-3} . This value is similar to the 200 mm w.e. found by Bales et al. [2001] and recent modeling efforts that produced an annual snowfall of 170 to 200 mm w.e. in the area near Summit [Fettweis, 2007; Ettema et al., 2009]. The annual mean latent heat contribution ($+6 \text{ mm}$ [Box and Steffen, 2001]) can only account for a small fraction of the difference. The intermittent MMCR measurements also indicate the same incongruity.

There are several potential contributions to this discrepancy. One is the only additional source of mass contained in equation (3), the redistribution of snow by wind below the measurement height of the POSS ($\sim 6 \text{ m}$). Quantifiable direct observations and modeling studies of drifting and blowing snow over Greenland are very sparse. However, Lenaerts et al. [2012] found that the net snow transport due to wind in the interior region of Greenland near Summit is quite small (a few mm w.e. per year at most) and is actually a net removal. Furthermore, Cullen et al. [2014] found good agreement between their surface mass balance model with no wind redistribution and the surface height measurements from the stake field at Summit, providing further guidance that the net effect of blowing snow must be small in this region.

Another potential source of error is the uncertainty in ΔH measurements. The mean ΔH of 71 cm agrees well with values found in other studies for areas near Summit, determined from methods including stake fields, snow pits, ice and firn cores, and acoustic ranging [Steffen and Box, 2001; Dethloff et al., 2002; Dibb and

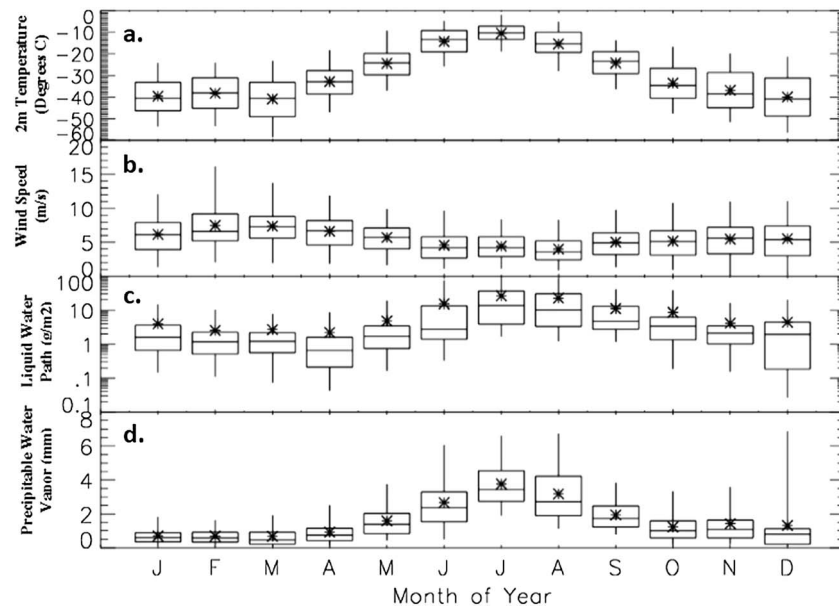


Figure 6. Monthly box-and-whisker plots for (a) 2 m temperature, (b) 10 m wind speed, (c) liquid water path, and (d) precipitable water vapor observed at Summit (June 2010 to October 2012).

Fahnestock, 2004). It is conceivable that ΔH near Summit is slightly enhanced compared to nearby undisturbed areas due to spatial drifting effects caused by the camp itself. However, this effect is likely small [e.g., *Dibb and Fahnestock, 2004*] and could act in either direction.

Uncertainty in the remote sensor reflectivity measurements can be a factor, yet the agreement between the two independent radars is quite good. Based on the estimated uncertainty of the POSS detailed in section 4 (a factor of 2 for reflectivity), the mean annual derived snowfall could be as high as 185 mm w.e. However, the mass difference is still too large to be fully explained by uncertainty in the POSS and MMCR reflectivity measurements alone. Therefore, a significant portion of the difference must be related to the retrievals used to derive snowfall from reflectivity. Uncertainty in the coefficients used in the Z_e - S relationships may be as large as a factor of 2, so the uncertainty in derived snowfall rate could be substantial [*Matrosov, 2007*]. Such uncertainties are likely at Summit as the specific snowfall retrievals employed here were designed for snow properties at midlatitudes and may not be fully representative of snow in a high altitude, extremely cold Arctic environment like Summit. Under these conditions individual crystal densities may be smaller, habits can be different, and size distributions may be unique. These crystal differences can affect the scattering properties that relate measured reflectivity to the snowfall amount. Unfortunately, little quantitative information is available on snow crystal properties and distributions at Summit. Potential avenues for addressing these issues and potentially adapting the retrievals in the future are given in section 6. However, in spite of the apparent mass underestimates, the retrievals do provide important insight into the temporal evolution of snowfall that can be used alongside other measurements to study the processes that influence snowfall.

5.2. Influence of Local Meteorology

The strong seasonal variability in snowfall at Summit suggests seasonally varying influences from meteorological conditions. Figure 6 shows the seasonal cycles of four parameters that may play roles in snowfall variability: 2 m temperature, 10 m wind speed, LWP, and PWV. Temperature, LWP, and PWV show maxima in the summer and a general minimum throughout the rest of the year, while wind speed has a summertime minimum. These annual cycles provide important context for the following discussion.

The direction from which air masses impinge on Summit can influence snowfall. Figure 7 shows four panels that relate snowfall to seasonal variations in local 10 m wind direction. The dominant wind direction throughout the year is southeasterly to southwesterly, with a more dominant westerly component in

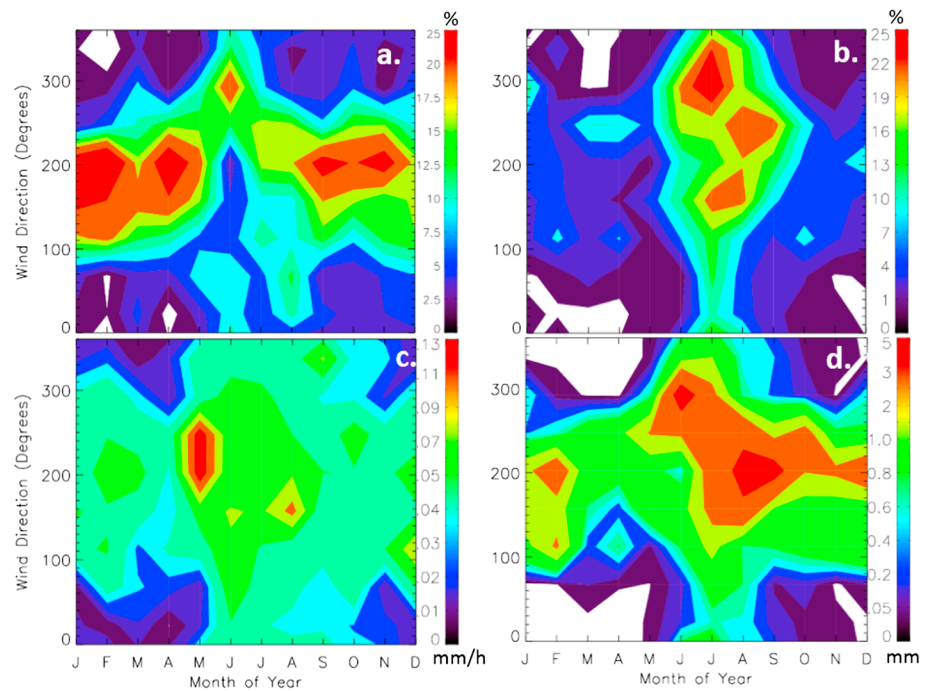


Figure 7. (a) The occurrence fraction of 10 m wind directions normalized by month of year. (b) The percent of time it was snowing as a function of 10 m wind directions and month of year. (c) The mean snowfall rate when it was snowing as a function of 10 m wind directions and month of year. (d) The total water equivalent snowfall as a function of 10 m wind direction and month of year derived by combining Figures 7a–7c. Wind direction bin sizes are 15°.

June (Figure 7a). Figure 7b shows the percentage of time it was snowing when the wind was blowing from a given direction for each month. A midsummer maximum is seen in all wind directions. Outside of June, July, and August, there is less than 5% snowfall occurrence for all wind directions that have a northerly component. Figure 7c considers the mean snowfall rate as a function of month and wind direction when it is snowing. Again, there is a directional dependence of snowfall, with very low rates when the wind has any northerly component for November through May. For all other wind directions and seasons, rates are approximately within a factor of 2, with the highest rates for southerly winds in May through September. The large maximum in May is likely not representative, but instead, the result of one or two intense snowfall events during the measurement period occurring in a month that sees little snowfall in general.

Combining Figures 7a–7c gives Figure 7d, which highlights the most important parameter, mass. This plot confirms that nearly all of the snowfall mass at Summit between September and May occurs when the local wind direction has a southerly component. This is the result of three factors: the low occurrence of northerly wind directions during these months, a low occurrence of snowfall when the wind does have a northerly component, and minimal snowfall rates during snowfall occurring under northerly winds. In summer, some mass results from conditions with northerly winds. The seasonal cycle of snowfall mass from northerly winds is likely a result of the presence of winter sea ice surrounding all of Greenland except the North Atlantic Ocean to the south. The diminished directional dependence in summer may be related to the springtime retreat of the sea ice surrounding Greenland, exposing open ocean in most directions.

Another local variable that may be part of the linkage to open water is the moisture content of the air above Summit. The atmospheric boundary layer at Summit (and presumably over much of the GIS) is quite shallow, often less than 100 m in depth and frequently contains a very cold, surfaced-based inversion [Miller *et al.*, 2013; Shupe *et al.*, 2013]. In part because of this stratification, the regional ice sheet itself is likely not an adequate source of moisture for cloud and precipitation formation. As a result of this decoupling, most of the snowfall at Summit must be generated by clouds that are formed and sustained by moisture that was advected in aloft from afar. To examine moisture content available to form clouds and produce precipitation the total vertical integrated column of water vapor, or the precipitable water vapor (PWV), derived from microwave radiometers is used. Figure 8a (and Figure 6d) shows monthly values of PWV

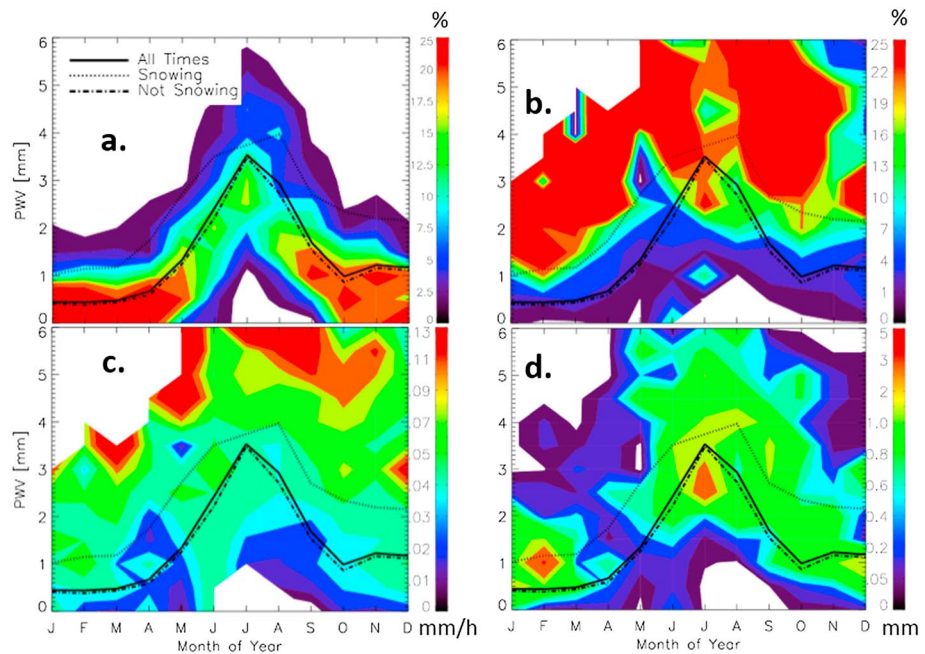


Figure 8. (a) The occurrence fraction of PWV values normalized by month of year. (b) The percent of time it was snowing as a function of PWV and month of year. (c) The mean snowfall rate when it was snowing as a function of PWV and month of year. (d) The total water equivalent snowfall as a function of PWV and month of year derived by combining Figures 8a–8c. PWV bin sizes are 0.5 mm. The black lines in each panel denote the mean PWV for all times, when it was snowing, and when it was not snowing.

peaking above 3 mm in summer and generally less than 1.5 mm throughout the remainder of the year. Not surprisingly, the odds of snowfall occurring during any given month increase with increasing PWV, particularly when PWV is above its monthly mean (Figure 8b). With the exception of July and August when PWV is at its annual maximum, snowfall occurs less than 5% of the time when PWV is below its monthly mean. Additionally, most appreciable snowfall rates occur under the same constraints (Figure 8c). However, large PWV values are relatively infrequent, such that the total snowfall mass in each month (Figure 8d, which combines Figures 8a–8c) is composed of a few large snowfall events combined with many weaker snowfall events. As a result, most snow mass occurs when PWV is near or slightly above its monthly mean. Remarkably, appreciable snowfall mass can even occur with PWV less than 1 mm in winter.

Figure 6c shows the summertime maximum in cloud liquid water path (LWP) corresponding with higher temperatures and more moisture availability. An intriguing unknown is whether or not the amount of cloud water has any influence on snowfall, as LWP can only indirectly influence snowfall through cloud microphysical processes. As 2 m temperature increases, larger values of LWP are more frequently observed (Figure 9a). For a given LWP, snowfall occurrence fraction increases with increasing T until -15°C , where snowfall occurrence is maximized at all LWPs (Figure 9b). This temperature coincides with the maximum saturation vapor pressure difference between water and ice. While there is some indication of more frequent snowfall at higher LWP (Figure 9b), the snowfall rate when it is snowing does not appear strongly dependent on LWP (Figure 9c) and actually appears to have a weak maximum for $\text{LWP} \sim 15\text{--}30\text{ g/m}^2$ at all temperatures. On the other hand, the snowfall rate when it is snowing clearly increases with temperature at all LWPs. Figure 9d, which combines the information from the other three panels, shows that, on average, LWP is lower when it is snowing compared to times when it is not snowing and most mass occurs when LWP is below its mean for all temperatures. The snowfall mass distribution decreases at higher LWP, in large part due to the infrequent occurrence of high LWP. Together, these results indicated that (1) LWPs are quite small at Summit, (2) more efficient precipitation appears to coincide with periods where the Bergeron process has acted to enhance ice growth while depleting liquid water, and/or (3) ice-phase precipitation systems and processes can be quite important for snowfall at Summit.

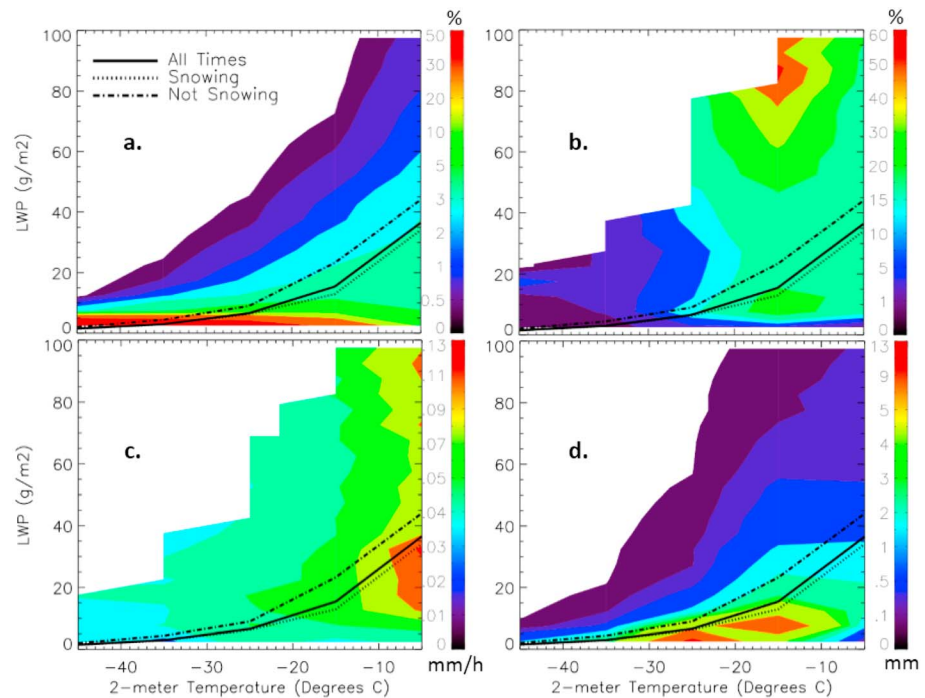


Figure 9. (a) The occurrence fraction of LWP values normalized by temperature. (b) The percent of time it was snowing as a function of LWP and temperature. (c) The mean snowfall rate when it was snowing as a function of LWP and temperature. (d) The total liquid equivalent snowfall as a function of LWP and temperature derived by combining Figures 9a–9c. Bins for LWP are 5 g/m^2 and for temperature are 10° . The black lines in each panel denote the mean LWP for all times, when it was snowing, and when it was not snowing.

6. Conclusions

To further the understanding of the central GIS mass budget, measurements of snowfall rate at Summit between September of 2010 and October 2013 are examined. POSS reflectivity and snowfall rate measurements were compared to those of the co-located MMCR, an instrument with a generally well-characterized uncertainty. The POSS was found to agree with the MMCR, both in terms of reflectivity and retrieved snowfall rate. Overall, the POSS was found to have an uncertainty that is likely less than 3 dB for reflectivity. Such an error implies an uncertainty of slightly less than a factor of 2 for snowfall retrievals due to the reflectivity, which is consistent with past evaluations of POSS-based retrievals and similar to MMCR-based retrieval uncertainties.

Using the POSS and MMCR measurements, the annual cycle of snowfall shows a clear summertime maximum and a spring minimum. The annual mean snowfall measured by the POSS (MMCR) was 92.5 mm w.e. (88.8 mm w.e.). A comparison to the seasonal cycle of surface height change showed similar seasonal patterns, although the variability is dampened and a one or two month time lag exists. A cumulative time series of surface height change and snowfall shows that while surface height increases at a relatively steady rate throughout the year, snowfall occurs in two distinct regimes. Snowfall rate is higher by nearly a factor of 3 between June and October, compared to the rest of the year. The rate of surface height change sees just a 15% increase during this same timeframe in relation to the rest of the year. A relatively low correlation between snowfall and surface height change indicates that other factors like compaction (likely the main influence), latent heat flux, and the redistribution of snow by wind are also important contributors to the seasonal variability of surface height change. These factors combine to give a smaller amplitude seasonal cycle for accumulation relative to snowfall.

The observed cumulative snowfall, when combined with estimated latent heat processes (i.e., deposition) and characteristic snowpack density, totals less than half of the observed surface accumulation. Some portion of this difference may be due to spatial drifting effects near Summit itself or blowing snow, but the most significant factor contributing to this difference is the underestimation of snowfall as a result of

POSS and MMCR measurement and retrieval uncertainties. These retrievals were designed for midlatitude snowfalls and may not fully represent the unique snow crystal distributions present at Summit. Despite the discrepancy between the ground-based remote sensors and in situ surface height change measurements, the POSS and MMCR provide snowfall data at a much higher temporal resolution that can be used for linking snowfall with system processes and meteorological events. Moreover, after further studies, the instantaneous snowfall estimates could be effectively “calibrated” in time using the stake field data. For example, an approximate doubling of snowfall retrievals by the POSS and MMCR would largely correct for the low bias. To help address these retrieval issues, the suite of ICECAPS precipitation instruments was expanded in summer 2014 to include important new perspectives from a hot plate precipitation gauge [Rasmussen *et al.*, 2011], which offers a high time resolution estimate of surface mass accumulation and a Multi-Angle Snowflake Camera, which can provide insight into the distribution of crystal shapes at Summit.

Snowfall at Summit, including occurrence, total, and rate, was found to be closely linked with local wind direction. Outside of the summer months, little snowfall accumulates when wind directions do not contain a southerly component. This relationship is believed to be linked to the seasonally changing sea ice coverage of the area immediately surrounding Greenland. Likewise, a dependence of snowfall on PWV is seen. Snowfall occurrence and rates are drastically higher when PWV exceeds its monthly mean value, consistent with snowfall being linked to moist air masses that are influenced by nearby, ice-free ocean. Cloud LWP is shown to have little relation to snowfall occurrence, with most snowfall occurring under conditions with little to no liquid water. However, snowfall generally increases with temperature, perhaps related to the increase in moisture availability. Interestingly, at any temperature, the LWP is generally smaller during snowfall than when snow is not occurring. Clearly, ice-phase precipitation processes are quite important for snowfall at Summit.

While the meteorological connections and snowfall analysis discussed here are local to Summit, they may offer broader insights into Greenlandic mass balance processes. Future work can utilize this snowfall data set, within the context of other ICECAPS instruments and collaborative projects at Summit, to develop a process-level understanding of precipitation as it relates to clouds, isotopic signatures, atmospheric stability, and others. These measurements can also be linked with satellite observations and/or model reanalysis products to examine and quantify spatial precipitation patterns impacting the central Greenland Ice Sheet.

Acknowledgments

All data sets used in these analyses are available via the Advanced Cooperative Arctic Data and Information Service (ACADIS), which is supported by the National Science Foundation, at www.aoncadis.org. Information on specific data sets can be found by searching on the keyword “ICECAPS.” This research was funded by the U.S. National Science Foundation under grants PLR1303879 and PLR1314156. The POSS was provided to the project by Environment Canada. The authors are grateful for comments from Sergey Matrosov and other collaborators on the ICECAPS project, including David Turner, Von Walden, Ralf Bennartz, and a large team of students, engineers, and science technicians. Joe McConnell and Roger Bales provided the stake field measurements, while NOAA Global Monitoring Division provided near-surface meteorological measurements.

References

- Albert, M. R., and E. F. Shultz (2002), Snow and firn properties and air-snow transport processes at Summit, Greenland, *Atmos. Environ.*, *36*, 2789–2797.
- Alley, R. B., P. U. Clark, P. Huybrechts, and I. Joughin (2005), Ice-sheet and sea-level changes, *Science*, *310*, 456–460.
- Arthern, R. J., D. G. Vaughan, A. M. Rankin, R. Mulvaney, and E. R. Thomas (2010), In situ measurements of Antarctic snow compaction compared with prediction of models, *J. Geophys. Res.*, *115*, F03011, doi:10.1029/2009JF001306.
- Bales, R. C., J. R. McConnell, E. Mosley-Thompson, and B. Csatho (2001), Accumulation over the Greenland ice sheet from historical and recent records, *J. Geophys. Res.*, *106*, 33,813–33,825, doi:10.1029/2001JD900153.
- Box, J. E., and K. Steffen (2001), Sublimation on the Greenland ice sheet from automated weather station observations, *J. Geophys. Res.*, *106*, 33,965–33,981, doi:10.1029/2001JD900219.
- Campos, E., and I. Zawadzki (2000), Instrumental uncertainties in Z-R relations, *J. Appl. Meteorol.*, *39*, 1088–1102.
- Cullen, N. J., T. Molg, J. Conway, and K. Steffen (2014), Assessing the role of sublimation in the dry snow zone of the Greenland ice sheet in a warming world, *J. Geophys. Res. Atmos.*, *119*, 6563–6577, doi:10.1002/2014JD021557.
- Dethloff, K., M. Schwager, J. H. Christensen, S. Kiilsholm, A. Rinke, W. Dorn, F. Jung-Rothenhauser, H. Fischer, S. Kipfstuhl, and H. Miller (2002), Recent Greenland accumulation estimated from regional climate model simulations and ice core analysis, *J. Clim.*, *15*, 2821–2832.
- Dibb, J. E., and M. Fahnestock (2004), Snow accumulation, surface height change, and firn densification at Summit, Greenland: Insights from 2 years of in situ observation, *J. Geophys. Res.*, *109*, D24113, doi:10.1029/2003JD004300.
- Ettema, J., M. R. van den Broeke, E. van Meijgaard, W. J. van de Berg, J. L. Bamber, J. E. Box, and R. C. Bales (2009), Higher surface mass balance of the Greenland ice sheet revealed by high-resolution climate modeling, *Geophys. Res. Lett.*, *36*, L12501, doi:10.1029/2009GL038110.
- Fettweis, X. (2007), Reconstruction of the 1979–2006 Greenland ice sheet surface mass balance using the regional climate model MAR, *Cryosphere*, *1*, 21–40.
- Fichefet, T., C. Poncin, H. Goosse, P. Huybrechts, I. Janssens, and H. Le Treut (2003), Implications of changes in freshwater flux from the Greenland ice sheet for the climate of the 21st century, *Geophys. Res. Lett.*, *30*(17), 1911, doi:10.1029/2003GL017826.
- Fujiyoshi, Y., T. Endoh, T. Yamada, K. Tsuboki, Y. Tachibana, and G. Wakahama (1990), Determination of Z-R relationship for snowfall using a radar and high sensitivity snow gauges, *J. Appl. Meteor.*, *29*, 147–152.
- Gregory, J. M., and P. Huybrechts (2006), Ice-sheet contributions to future sea-level change, *Philos. Trans. R. Soc. London A*, *364*, 1709–1731.
- Huang, G.-J., V. N. Bringi, D. Moisseev, W. A. Petersen, L. Bliven, and D. Hudak (2015), Use of 2D-video disdrometer to derive mean density-size and Ze-SR relations: Four snow cases from the light precipitation validation experiment, *Atmos. Res.*, *153*, 34–48.
- Jacobi, H., R. C. Bales, R. C. Honrath, M. C. Peterson, J. E. Dibb, A. L. Swanson, and M. R. Albert (2004), Reactive trace gases measured in the interstitial air of surface snow at Summit Greenland, *Atmos. Environ.*, *38*, 1687–1697.

- Krabill, W., W. Abdalati, E. Frederick, S. Manizade, C. Martin, J. Sonntag, R. Swift, R. Thomas, W. Wright, and J. Yungel (2000), Greenland Ice Sheet: High-elevation balance and peripheral thinning, *Science*, *289*, 428–430.
- Lenaerts, J. T. M., M. R. van den Broeke, J. H. van Angelen, E. van Meijgaard, and S. J. Déry (2012), Drifting snow climate of the Greenland Ice Sheet: A study with a regional climate model, *Cryosphere*, *6*, 891–899.
- Liljegren, J. C. (1999), Automatic self-calibration of ARM microwave radiometers, in *Microwave Radiometry and Remote Sensing of the Earth's Surface and Atmosphere*, edited by P. Pampaloni and S. Palosciam, pp. 433–443, VSP Press.
- Liu, G. (2008), Deriving snow cloud characteristics from CloudSat observations, *J. Geophys. Res.*, *113*, D00A09, doi:10.1029/2007JD009766.
- Macke, A., J. Mueller, and E. Raschke (1996), Single scattering properties of atmospheric ice crystals, *J. Atmos. Sci.*, *53*, 2813–2825.
- Matrosov, S. Y. (1992), Radar reflectivity in snowfall, *IEEE Trans. Geosci. Remote Sens.*, *30*, 454–461.
- Matrosov, S. Y. (1998), A dual-wavelength radar method to measure snowfall rate, *J. Appl. Meteorol.*, *37*, 1510–1521.
- Matrosov, S. Y. (2007), Modeling backscatter properties of snowfall at millimeter wavelengths, *J. Atmos. Sci.*, *64*, 1727–1736.
- Matrosov, S. Y., M. D. Shupe, and I. V. Djalalova (2008), Snowfall retrievals using millimeter-wavelength cloud radars, *J. Appl. Meteorol.*, *47*, 769–777.
- Matrosov, S. Y., C. Campbell, D. Kingsmill, and E. Sukovich (2009), Assessing snowfall rates from X-band radar reflectivity measurements, *J. Atmos. Oceanic Technol.*, *26*, 2324–2339.
- Miller, N. B., D. D. Turner, R. Bennartz, M. D. Shupe, M. S. Kulie, M. P. Cadeddu, and V. P. Walden (2013), Surface-based inversions above central Greenland, *J. Geophys. Res. Atmos.*, *118*, 495–506, doi:10.1029/2012JD018867.
- Mischenko, M. I. (2000), Calculation of the amplitude matrix for a nonspherical particle in a fixed orientation, *Appl. Opt.*, *39*, 1026–1031.
- Moran, K., B. Martner, M. Post, R. Kropfli, R. Welsh, and K. Widener (1998), An unattended cloud profiling radar for use in climate research, *Bull. Am. Meteorol. Soc.*, *79*, 443–455.
- Ohmura, A., and N. Reeh (1991), New precipitation and accumulation maps for Greenland, *J. Glaciol.*, *37*(125), 140–148.
- Purcell, E. M., and C. R. Pennypacker (1973), Scattering and absorption of light by nonspherical dielectric grains, *Astrophys. J.*, *186*, 705.
- Rahmstorf, S. (1995), Bifurcations of the Atlantic thermohaline circulation in response to change in the hydrological cycle, *Nature*, *378*, 145–149.
- Rahmstorf, S. (2000), The thermohaline ocean circulation: A system with dangerous thresholds?, *Clim. Change*, *46*, 247–256.
- Rasmussen, R. M., J. Hallett, R. Purcell, S. D. Landolt, and J. Cole (2011), The Hotplate precipitation gauge, *J. Atmos. Oceanic Technol.*, *28*, 148–164.
- Rose, T., S. Crewell, U. Löhnert, and C. Simmer (2005), A network suitable microwave radiometer for operational monitoring of the cloudy atmosphere, *Atmos. Res.*, *75*, 183–200.
- Shepherd, A., et al. (2012), A reconciled estimate of ice-sheet mass balance, *Science*, *338*(6111), 1183–1189.
- Sheppard, B. E. (1990), Measurement of raindrop size distributions using a small Doppler radar, *J. Atmos. Oceanic Technol.*, *7*, 255–268.
- Sheppard, B. E., and P. I. Joe (1994), Comparison of raindrop size distribution measurements by a Joss-Waldvogel disdrometer, a PMS 2DG spectrometer, and a POSS Doppler radar, *J. Atmos. Oceanic Technol.*, *11*, 874–887.
- Sheppard, B. E., and P. I. Joe (2000), Automated precipitation detection and typing in winter: A two-year study, *J. Atmos. Oceanic Technol.*, *17*, 1493–1507.
- Sheppard, B. E., and P. I. Joe (2008), Performance of the Precipitation Occurrence Sensor System as a precipitation gauge, *J. Atmos. Oceanic Technol.*, *25*, 196–212.
- Shiina, T., M. Kubo, and K. Muramoto (2010), Z-R relation for snowfall using two small Doppler radars and snow particle images, in *2010 IEEE International Geoscience and Remote Sensing Symposium*, pp. 4122–4125, IEEE, Honolulu, Hawaii.
- Shupe, M. D. (2007), A ground-based multiple remote-sensor cloud phase classifier, *Geophys. Res. Lett.*, *34*, L22809, doi:10.1029/2007GL031008.
- Shupe, M. D., et al. (2013), High and dry: New observations of tropospheric and cloud properties above the Greenland Ice Sheet, *Bull. Am. Meteorol. Soc.*, *94*, 169–186.
- Spencer, M., R. Alley, and T. Creyts (2001), Preliminary firn-densification model with 38-site dataset, *J. Glaciol.*, *47*(159), 671–676.
- Steffen, K., and J. Box (2001), Surface climatology of the Greenland ice sheet Greenland Climate Network 1995–1999, *J. Geophys. Res.*, *106*, 33,951–33,964, doi:10.1029/2001JD900161.
- Stouffer, R. J., et al. (2006), Investigating the causes of the response of the thermohaline circulation to past and future climate changes, *J. Clim.*, *19*, 1365–1387.
- Thomas, R., T. Atkins, B. Csatho, M. Fahnestock, P. Gogineni, C. Kim, and J. Sonntag (2000), Mass balance of the Greenland Ice Sheet at high elevations, *Science*, *289*, 426–428.
- Turner, D. D., S. A. Clough, J. C. Liljegren, E. E. Clothiaux, K. Cady-Pereira, and K. L. Gaustad (2007), Retrieving liquid water path and precipitable water vapor from Atmospheric Radiation Measurement (ARM) microwave radiometers, *IEEE Trans. Geosci. Remote Sens.*, *45*, 3680–3690.
- van den Broeke, M., J. Bamber, J. Ettema, E. Rignot, E. Schrama, L. J. van de Berg, E. van Meijgaard, I. Velicogna, and B. Wouters (2009), Partitioning recent Greenland mass loss, *Science*, *326*, 984–986.
- Wong, K. C. (2012), Performance of several present weather sensors as precipitation gauges, WMO. [Available at http://www.wmo.int/pages/prog/www/IMOP/publications/IOM-109_TECO2012/Session1/P1_30_Wong_Performance_Wx_Sensors_Precip_Gauges.pdf].